FRACTURE TOUGHNESS EVALUATION FROM TENSION AND CHARPY TYPE SPECIMENS BASED ON MICROMECHANICAL MATERIAL MODELS

D.-Z. SUN, W. BROCKS and W. SCHMITT
Fraunhofer-Institut für Werkstoffmechanik
Wöhlerstr. 11, D-7800 Freiburg, Germany

ABSTRACT

To relate micromechanical approaches to conventional fracture mechanics, dynamic tensile tests and instrumented impact tests with Charpy-V-notch specimens and precracked Charpy specimens (SENB) are performed and simulated. Two strain-rate dependent micromechanical models based on the modified Gurson flow function are compared by simulating different dynamically loaded specimens. The results indicate that the critical void volume fraction f_c and the charateristic length l_c are practically independent of strain rate and specimen geometry. The deformation and fracture behaviour of fracture mechanics specimens can be well calculated with the parameters determined from a tensile test and an instrumented Charpy-V test. The tunneling of the crack in the interior of the Charpy specimen is predicted in a satisfactory way by a three-dimensional analysis with the strain-rate dependent Gurson model.

KEYWORDS

Micromechanics, Gurson model, numerical simulation, ductile fracture, strain-rate effect, Charpy-V test, impact test, dynamic tensile test.

INTRODUCTION

Compared with conventional fracture mechanics concepts, micromechanical models have the advantage that the corresponding material parameters for ductile fracture can be transfered between different specimen geometries. Another advantage is that studying material failure with such models results in a better understanding of rupture processes, especially for inhomogeneous materials, and thus indicates the best way to optimize material toughness. Both models adapted in this study are based on a flow function derived by Gurson [1] and modified by Needleman and Tvergaard [2,3] to analyze fracture behaviour in notched bars and to predict the onset of crack growth in cracked specimens. The description of ductile rupture processes, void nucleation, growth and coalescence, is incorporated in the constitutive relations. The applicability of this model was verified by Sun et al. [4,5] by predicting the results of notched bar tests using parameters determined from smooth tensile tests. Ductile crack extension in various types of precracked specimens of a given material was successfully calculated by using only one set of parameters and an additional length parameter.

Since the variation of strain rate influences both the material flow behaviour and the fracture processes, two questions have to be answered before a micromechanical model can be used for dynamic loading. First, which material model does appropriately describe the effects of strain-rate hardening, including the thermal softening effects. Second, do the micromechanical parameters depend on strain rate, and how can they be determined. To solve these problems, both a theoretical and an empirical strain-rate dependent material model based on the modified Gurson flow function were implemented in a commercial finite-element program. Static and dynamic tensile tests and instrumented impact tests with Charpy-V and SENB specimens were carried out. The applicability of the micromechanical models to dynamic loading and the relation between the micromechanical approaches and conventional fracture mechanics concepts were systematically studied by simulating the specimens under different loading situations.

STRAIN-RATE DEPENDENT GURSON MODELS

One of the material models describing the strain-rate dependency of the flow stress was developed by Macherauch and Vöhringer [6] considering of thermal activation processes. In the present work this theoretical model is denoted "model 1". Details about its parameters may be found in [7]. The second model was introduced by Pan et al. [8]:

$$\sigma = \sigma_o(\varepsilon)\,[1-\beta(T-T_o)]\left(\frac{\dot{\varepsilon}_p}{\dot{\varepsilon}_o}\right)^m , \quad m << 1 \quad (model\ 2) \qquad (1)$$

$\dot{\varepsilon}_o$ and T_o are a reference strain rate and reference temperature, respectively, σ_o denotes the flow stress measured at $\dot{\varepsilon}_o$ and T_o. β is a material dependent parameter. During the plastic deformation nearly all plastic work is converted into heat. If the strain rate in a test exceeds a critical strain rate, the heat transfer during deformation is negligible, the test is adiabatic. The temperature increase for an adiabatic test can be calculated from the energy balance. The adiabatic heating results in a softening of the material due to the reduction of the yield stress. This effect can be taken into account in both material models.

Both strain-rate dependent models have been combined with the modified Gurson model [3,9] which is based on a plastic potential applicable to porous solids given by

$$\phi = \frac{3\sigma'_{ij}\,\sigma'_{ij}}{2\sigma^2} + 2q_1 f^*\cosh\left(\frac{\sigma_{kk}}{2\sigma}\right) - [1+(q_1 f^*)^2] = 0 \ . \qquad (2)$$

σ denotes flow stress of the matrix material which depends on strain, strain rate and temperature. f^* is a function of the void volume fraction and was suggested by Needleman and Tvergaard [2] to simulate the rapid loss in stress carrying capacity of the material caused by void coalescence. In an analysis using the modified Gurson model initiation and propagation of the crack are intrinsic results of the local softening due to void coalescence which begins when a critical void volume fraction f_c is exceeded over a characteristic distance l_c [5].

EXPERIMENTAL PROCEDURES

The experiments were carried out with the pressure vessel steel 22NiMoCr3 7 (≈ ASTM A 508 Cl 2) at room temperature. The diameter and the gage length of smooth tensile bars are 6 mm and 30 mm respectively. While in the static tensile tests an initial strain rate $\dot{\varepsilon}=2\times10^{-4}$/s was obtained in a servohydraulic testing machine, in the dynamic tests an initial strain rate $\dot{\varepsilon}$=50/s was achieved by performing the tests in a drop weight tower with an impacting mass of 273 kg and with an impact velocity of 2 m/s. For the evaluation of true stress vs. true strain curves the specimens were photographed during the impact tests with a 24-spark Cranz-Schardin high speed camera [10]. Fig. 1 shows a series of those photographs from which the elongation, the area reduction and the necking radius were measured.

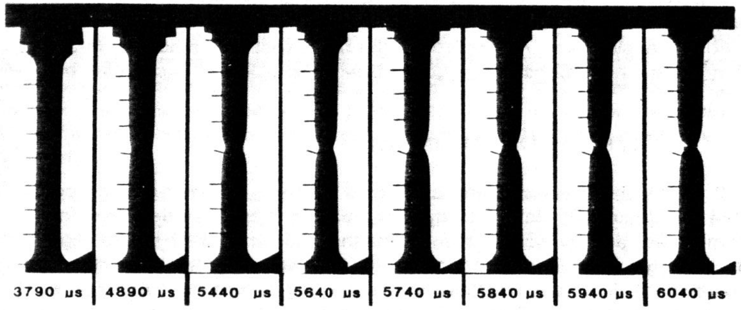

FIG. 1—Development of the necking photographed during a dynamic tensile test

Two series of instrumented impact tests with Charpy-V specimens and precracked Charpy specimens (SENB) were performed with impact velocities between 0.5 and 1.2 m/s. The hammer-load was measured by means of strain gages and recorded as a function of the time. The time dependent displacement of the hammer was integrated from the load signal. The SENB specimens were side-grooved (10% on each side) and the relative crack length was about a/W=0.53. For the evaluation of an experimental dynamic J_R-curve different amounts of ductile crack extension were achieved by variation of the impact velocity. Static fracture mechanics tests were carried out using CT25 specimens with 20% side grooves and a/W=0.6 and the J_R-curve was determined using the partial unloading technique.

NUMERICAL METHODS

The material parameters describing the strain-rate hardening were evaluated from the tensile tests. For model 2 the parameter m=0.0175 was obtained by inserting the stresses at maximum load and the corresponding strain rates into equation 1. The value β=0.0004/K was evaluated from the static yield stresses measured at two different temperatures (293° K and 493° K). The parameters for the modified Gurson model except f_c were taken from Ref [3] and a previous study [5]. The critical void fraction f_c=0.045 was determined by fitting the sudden drop in the numerical load vs. diameter change curve of static tensile test with the measured displacement at rupture. It was assumed that the material is initially void free. The void fraction at fracture was taken to be f_f=0.2.

The complex loading and support situation of the Charpy tests including sliding and friction at the anvils makes the numerical simulation more difficult. An acceptable solution was found by modelling the supports of the specimen with contact surfaces and the hammer with gap elements. An important step for the simulation of cracked specimens with micromechanical models is the choice of the element size in the crack tip region and the introduction of a characteristic length because of the great gradient of the stress field at the crack tip. This was achieved by defining one element at the crack tip as a damage cell and starting the acceleration of damage at the different integration points in the element at the same time. The element size was determined by fitting the measured load versus displacement curve of a CT specimen. This element size representing l_c was also used for the Charpy-V and SENB specimens.

The simulations of the side-grooved CT and SENB specimens were performed under the assumption of plane strain conditions. For the Charpy-V specimen a combined 2D/3D model was applied: The region around the notch root was modelled in 3D, the remaining part in plane stress. Constraint equations were established to combine both parts.

EFFECTS OF STRAIN RATE

Fig. 2 shows the measured and calculated load vs. diameter-change curves of smooth tensile specimens for static and dynamic loading. For small deformations the measured dynamic loads are significantly higher than the static ones. With increasing deformation the static and dynamic curves fall together. This effect can only be partly explained by the adiabatic softening mainly occuring in the necking part of the dynamic tensile specimens because the measured β-value is just one half of that β-value which yields a good agreement of the numerical predictions with the measured load vs diameter change curve. The results of three simulations based on model 2 show that for small deformations up to maximum load the adiabatic effect is negligible, but it becomes more and more obvious with increasing deformation.

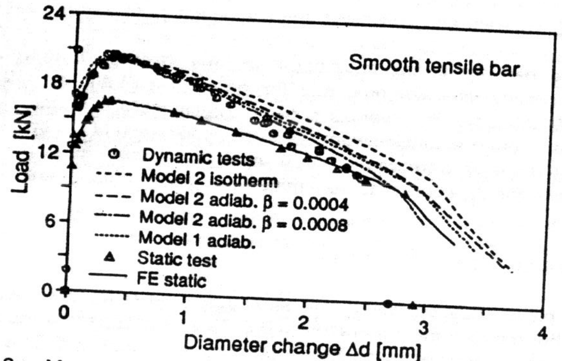

FIG. 2—Measured and calculated load vs. diameter change curves of smooth tensile specimens under static and dynamic loading

Fig. 2 shows that the final rupture of the dynamic tensile specimens can be predicted in a satisfactory way with those micromechanical parameters used for the simulation of the static tests, if the plastic deformation behaviour of the specimen is covered well enough. This means that the critical damage parameter f_c is practically independent of strain rate.

In order to go further into the question of the strain-rate dependency of the micromechanical parameters finite element calculations of a cell model have been performed. In this model the continuum is considered to consist of a periodic assemblage of hexagonal cylindrical unit cells (approximated by spherical cylinders which allow for a simple axisymmetric calculation). Every unit cell contains a spherical hole and is subject to homogeneous radial and axial displacements. Special loading conditions were applied to the surface of the cylinder to keep the "macroscopic" triaxiality T constant during the loading process [11]. The axial displacement was increased until plastic strain localized in the net section.

The macroscopic effective stress responses which were obtained for the cell model have been compared with the predictions of the semi-analytical solutions of the modified Gurson model. The Gurson parameters were chosen in a way that the predictions fit the cell model results of the static calculations best. Fig. 3a shows that one set of parameters can be found which gives a satisfactory prediction independent of the triaxiality. Visco-plastic calculations at high strain rates show that the strain rate does not affect the void growth whereas the macroscopic effective stress rises and localization is slightly retarded, Fig. 3b. Nevertheless, the assumption that the Gurson parameters do not depend on the strain rate still gives a satisfactory agreement between the cell modell results at high strain rates and the Gurson model.

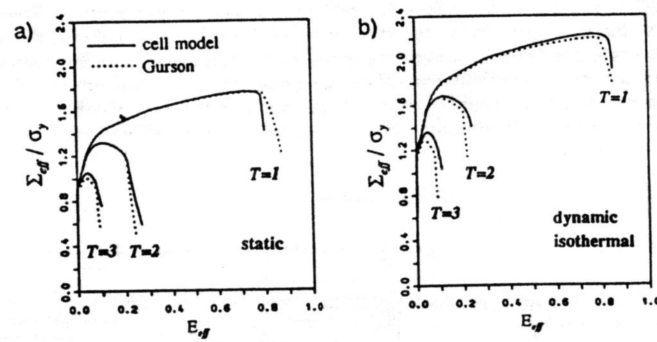

FIG. 3—Macroscopic effective stress vs. strain relationship from the cell model compared with that from Gurson model using the same f_c for static (a) and dynamic (b) loading

APPLICATION TO INSTRUMENTED CHARPY-V TESTS

Since the Charpy-V-notch impact test is more frequently used than dynamic tensile tests and fracture mechanics tests, it is desirable to determine the material parameters for the strain-rate dependent models directly from the Charpy-V test. A problem for the simulation of the Charpy-V specimen is that the stress state of this specimen can not be approximated by a two-dimensional model due to the absence of side grooves. Fig. 4 shows the load versus displacement curves calculated with different models in comparison with the experimental results. The material parameters obtained from the simulations of the tensile tests and a length parameter l_c determined from a compact tension test are used for all three finite-element models with identical in-plane element arrangements.

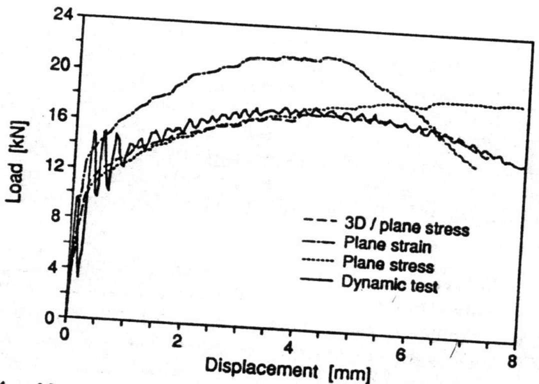

FIG. 4—Measured load versus displacement curve of a Charpy-V specimen in comparison with the curves calculated with 2D- and 3D-models

Evidently, the plane-strain model overestimates considerably the measured loads before crack initiation. Moreover, the calculated damage resulting in the crack extension develops too fast and the calculated loads fall steeply below the measured values. The plane-stress model delivers a good description of the global behaviour of the specimen up to maximum load. However, the crack initiation does not occur because the critical damage is not reached due to the low triaxiality of the stress state in the model. The combined 3D/2D model gives obviously a good solution in the whole deformation range.

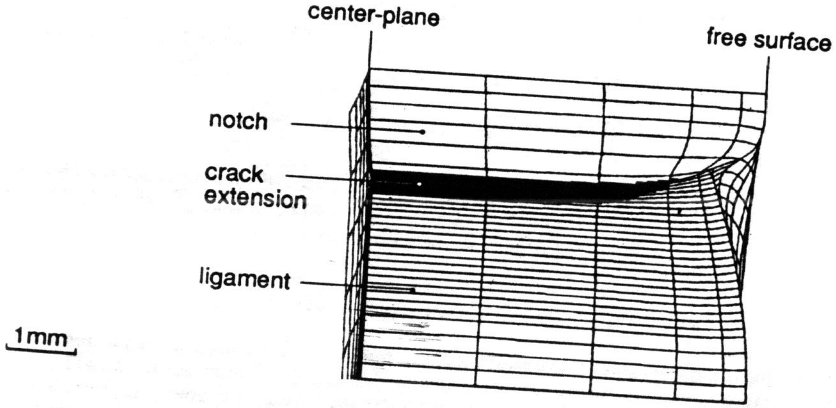

FIG. 5—Calculated deformation and crack extension of a Charpy-V specimen.

Fig. 5 displays a three-dimensional view of the deformed near-notch mesh on which the damage zone ($f \geq f_f$) is imposed. By comparison with the fracture surface of a Charpy-V specimen it becomes apparent that both the tunneling of the crack in the interior of the specimen and the side contraction are well predicted based on the micromechanical model.

RELATION TO FRACTURE MECHANICS CONCEPTS

An instrumented impact test with a SENB specimen was simulated using the micromechanical models with the very set of parameters as had been used for the simulation of the Charpy-V test. The calculated and measured dynamic J_R-curves are compared in Fig. 6, where the results for quasi-static loading are plotted as well. As expected, dynamic loading results in an increase of the ductile crack resistance of the material. A good agreement between numerical and experimental results is obtained overall for the impacted SENB specimens and up to a crack extension of 1 mm for the quasi-statically loaded CT-specimen. The deviation of the calculated J-values from the measured one for the CT specimen is mainly attributed to the scatter of the material strength.

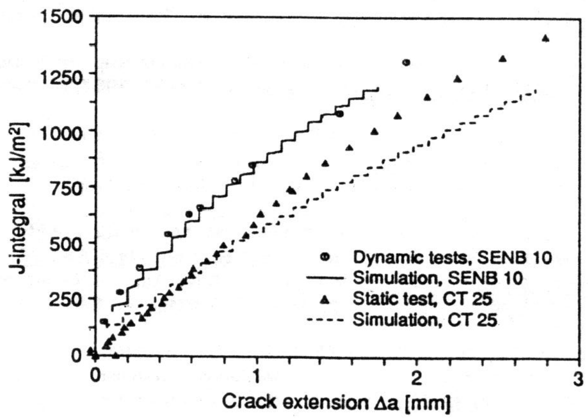

FIG. 6—Measured and calculated J_R-curves for static and dynamic loading

Although both the J-integral concept and the micromechanical models can be used to analyse the ductile crack extension for the applied specimen geometries, the parameters for the micromechanical models are also applicable for different geometries of specimens or components and loading conditions. Another interesting point found in the analyses of the specimens with different models is that in contrast to the dynamic tension tests the adiabatic softening does not play an important role in cracked specimens.

CONCLUSIONS

The strain rate hardening and adiabatic softening of the material under investigation can be sufficiently described by two different material models. The effect of adiabatic heating is more pronounced in dynamic tensile tests than in impact tests with fracture mechanics specimens. The critical void volume fraction f_c and the charateristic length l_c are practically independent of strain rate. They can be determined by simulating a tensile test with a smooth bar and an instrumented Charpy-V-notch test, respectively.

The static and dynamic J_R-curves calculated using the modified Gurson model are in good agreement with the measured ones. The tunneling of the crack observed experimentally in a Charpy-V specimen is well predicted by a three-dimensional simulation with the damage model covering rate-dependent stress-strain behaviour. The intense strain concentration and the low stress triaxiality in the region between the tunneled core and the side ligament provides a favourable condition for shear failure.

REFERENCES

[1] Gurson, A. L., "Continuum Theory of Ductile Rupture by Void Nucleation and Growth: Part I-Yield Criteria and Flow Rules for Porous Ductile Media," Journal of Engineering Materials and Technology, Vol.99, 1977, pp 2-15.

[2] Needleman, A. and Tvergaard, V., "An analysis of Ductile Rupture in Notched Bars," Journal of Mechanics and Physics of Solids, Vol. 32, 1984, pp 461-490.

[3] Needleman, A. and Tvergaard, V., "An analysis of Ductile Rupture Modes at a Crack Tip," Journal of Mechanics and Physics of Solids, Vol.35, 1987, pp 151-183.

[4] Sun, D.-Z., Siegele, D., Voss, B. and Schmitt, W., "Application of Local Damage Models to the Numerical Analysis of Ductile Rupture," Fatigue & Fracture of Engineering for Materials & Structures, Vol. 12, 1988, pp 201-212.

[5] Sun, D.-Z., Kienzler, R., Voss, B. and Schmitt, W., "Application of Micro-mechanical Models to the Prediction of Ductile Fracture," Fracture Mechanics: Twenty-Second Symposium (Volume II), ASTM STP 1131, eds. S. N. Atluri, J. C. Newman, Jr., I. S. Raju, and J.S. Epstein, American Society for Testing and Materials, Philadelphia, 1992, pp 368-378.

[6] Macherauch, E., Vöhringer, O., "Das Verhalten metallischer Werkstoffe unter mechanischer Beanspruchung," Zeitschrift für Werkstofftechnik, 9, 1978, pp 370-391.

[7] Sun, D.-Z., Hönig, A., Böhme, W., Schmitt, W., "Application of Micromechanical Models to the Analysis of Ductile Fracture under Dynamic Loading," Fracture Mechanics: 25th Volume, ASTM STP 1220, eds. F. Erdogan and Ronald J. Hartranft, to be published.

[8] Pan, J., Saje, M., Needleman, A., "Localization of Deformation in Rate Sensitive Porous Plastic Solids," International Journal of Fracture, Vol.21, 1983, pp 261-278.

[9] Needleman, A. and Tvergaard, V., "An Analysis of Dynamic Ductile Crack Growth in a Double Edge Cracked Specimen," International Journal of Fracture, Vol.49, 1991, pp 41-67.

[10] Böhme, W., Sun, D.-Z., Schmitt, W., Hönig, A., "Application of Micromechanical Material Models to the Evaluation of Charpy Tests", Advances in Local Fracture / Damage Models for the Analysis of Engineering Problems, AMD-Vol. 137, Editors: J.H. Giovanola, and A.J. Rosakis, 1992, pp 203-216.

[11] Brocks, W., Hönig, A., Sun, D.-Z., "Verification of the Transferability of Micro-Mechanical Parameters by Cell Model Calculations with Visco-Plastic Materials," Fourth International Symposium on Plasticity and Its Current Applications, Baltimore, MD, July 19-23, 1993.